ECOLOGICAL MODELLING 199 (2006) 53–63

available at www.sciencedirect.com

journal homepage: www.elsevier.com/locate/ecolmodel

A methodology for assessing departure of current plant communities from historical conditions over large landscapes

Brian M. Steele[a,*], Swarna K. Reddy[a], Robert E. Keane[b]

[a] Deptartment of Mathematical Sciences, University of Montana, Missoula, MT 59812, United States
[b] USDA Forest Service, Rocky Mountain Research Station, Fire Sciences Laboratory, P.O. Box 8089, Missoula, MT 59807, United States

ARTICLE INFO

Article history:
Received 22 September 2005
Received in revised form 26 May 2006
Accepted 13 June 2006
Published on line 8 August 2006

Keywords:
Multivariate statistical analysis
Outliers
Principal components analysis

ABSTRACT

Fire frequency and severity, and vegetation composition and structure have been altered across much of North America during the past century because of fire exclusion and other land management practices. The cumulative results are now recognized to be partly responsible for dramatic increases in wildland fire severity and declines in ecosystem health. In response, the Departments of Agriculture and Interior are developing a strategy for reducing fire hazard and restoring forest health. A key component of this strategy is the assessment of the departure of current plant communities from historical conditions. Assessing departure is difficult because of limited spatial coverage of data on successional class distribution prior to European settlement (historical) conditions. This article discusses a two-step approach to the problem that first generates data on historical vegetation composition and structure by simulating succession and disturbance processes under historical conditions, and then measures departure by comparing these simulated data to an observation on current conditions. The data are observations on high-dimensional multinomial categorical variables, and pose several problems that limit the usefulness of conventional statistical methods. We propose a method that constructs a linear approximation of the current observation vector from the simulated historic data, and measures the departure of the current observation vector by the length of the residual error vector. A simulation study indicates that this departure measure is substantially more sensitive than conventional outlier detection methods. Our methodology is demonstrated using a pilot region encompassing lands in Utah.

1. Introduction

Many forests and rangelands of North America experienced frequent, low severity fires prior to European settlement (circa 1900) (Wright and Heinselman, 1973; Heinselman, 1981; DeBano et al., 1998). Since European settlement, the frequency and severity of fire, vegetation composition and structure, and fuel loading have changed substantially (Ferry et al., 1995; Frost, 1998; Kolb et al., 1998; Arno et al., 2000; Keane et al., 2002b). Fire exclusion, livestock grazing, and logging, and generally, land management policies are widely attributed to these changes. A probable consequence of these changes are dramatic increases in the number, size, and intensity of wildfires in recent years (GAO, 2002). In response, Congress and the Executive Branch mandated the development of a National Fire Plan (www.fireplan.gov) for reducing fire hazard and restoring forest health. Through this vehicle, the Departments of Agriculture and Interior have been directed by Congress to

* *Corresponding author*. Tel.: +1 406 243 5396, fax: +1 406 243 2674.
E-mail address: steele@mso.umt.edu (B.S. Steele).
0304-3800/$ – see front matter © 2006 Elsevier B.V. All rights reserved.
doi:10.1016/j.ecolmodel.2006.06.016

develop a cohesive strategy for implementing the Plan (Laverty and Williams, 2000). These efforts, along with the passage of the Healthy Forests Restoration Act (www.healthyforests.gov), provide support for reducing fire hazard using silvicultural thinning and prescribed burning.

The Cohesive Strategy uses fire regime condition class as a key measure for implementing the National Fire Plan. Fire regime condition class measures the departure of current conditions from historical conditions with respect to fuel, fire regime, and vegetation (Laverty and Williams, 2000), and is used in part to direct funding and resources to those lands with the greatest need for restoration. However, assessing departure is difficult because data on historical conditions are extremely sparse (Keane et al., 2002a). Several strategies have been identified for quantifying local historical conditions (Landres et al., 1999), but the only practical strategy for assessing departure on a national scale is to generate historical data by spatially simulating plant community succession as disturbances across landscapes (Keane et al., 2002a; Landres et al., 1999).

The use of simulated data in ecology and resource management has become commonplace for large scale problems (Waring and Running, 1998). Examples include the analysis of net primary production (Jiang et al., 1999), forest planning (Bettinger et al., 2004), and nutrient cycling (Nour et al., 2006). In particular, succession and fire modeling has been an active area of ecological research for 3 decades (see Keane et al., 2004; Mladendoff and Baker, 1999). These models are now mature in their sophistication and accuracy, and limitations arising from model assumptions are widely understood (Botkin and Schenk, 1996; Keane et al., 2001). The current generation of successional models are spatially explicit, and model fire events as a function of topography, fuel, weather and prevailing wind direction (Keane et al., 2004). The subject of this article is the comparison of simulated historical and current observations, and departure assessment. The simulated data pose several statistical challenges common to data generated by automated collection devices and other recent technological innovations (Rao, 2004). These challenges include high-dimensional observations, massive data sets, and a lack of appropriate distributional models.

This article presents a statistical method of assessing the departure of current vegetation conditions from simulated historical conditions for each map unit in a landscape. The essence of the method is the comparison of an observation on the current distribution of successional classes to a simulated set of observations on the historical distribution of successional classes. The population of interest consists of the landscape units within geographic region, and an observation vector consists of the areal covers of each possible successional class within each observed potential vegetation class. Areal cover is quantified by the number of pixels within a landscape unit belonging to a particular potential vegetation class and successional class combination. As most of these class combinations are rare, or not present at a particular point in time, the data are observations on high-dimensional multinomial categorical variables dominated by zero counts. The tendency for many classes to be dominated by small counts implies that many conventional distribution-based statistical methods [e.g., the Chi-square test for homogeneity of proportions (Ott and Longnecker, 2001, Chapter 10)] are inappropriate for these data. Moreover, the historical data sets contain multiple linear dependencies, and so the data matrices are less-than-full rank. Most multivariate methods are based on using full rank data matrices and must be modified to accommodate a less-than-full rank data matrix.

These considerations motivate our approach. We construct a linear approximation of the current data vector using the historical data, and measure the departure of current from historical conditions by the approximation error. This is accomplished by using the singular value decomposition of the historic data matrix **X** to construct a projection matrix for the space spanned by the rows of **X**. Then, the departure of an observation vector X_0 is defined to be the length of the error, or residual vector associated with the projection of X_0 onto the space spanned by the rows of **X**. To determine the observed significance level, an empirical distribution of departure values is constructed by removing each simulated historical observation from **X** and computing its departure from the remaining data.

1.1. Background

Many federal land management agencies use a two-tier hierarchical plant community classification system (Anderson et al., 1998; Grossman et al., 1998) for describing large scale landscapes (for example, see Hessburg et al., 1999; Hann et al., 1998). The first tier, called the potential vegetation type, describes the biophysical conditions at a site by identifying the plant community that would exist if succession were to progress to the stable or climax community (Daubenmire, 1966; Pfister and Arno, 1980). The second tier of the classification system identifies the existing successional class at a site. Succession is the progression of plant communities from colonization to climax community. Usually, succession is described as a series of classes, and transition between classes is viewed as a deterministic process governed by species-specific environmental requirements, inter-species competition, and environmental conditions. In the plant community classification system, successional class is nested within potential vegetation type, and identifies the vertical structure and dominant overstory species. Fig. 1 shows an example of the successional pathways for a subalpine forest potential vegetation type found in Utah.

Disturbance events such as wildland fire interrupt succession and often modify the subsequent successional progression, or pathway. The resulting successional class and pathway depends on the disturbance severity. For example, a low intensity fire in a mid-successional forest class may remove understory trees leaving a single-strata overstory tree canopy that will progress to a two-tiered canopy, whereas a high intensity fire may produce a grass and shrub community that will progress towards a single-strata canopy. Low intensity fires tend to perpetuate some non-climax successional classes. For example, frequent fires in a grass and shrub community will prevent the establishment of an overstory, thereby maintaining the grass and shrub community. Mid-successional forests are also maintained by low intensity fires that eliminate climax tree species from the understory. On the other hand, early-successional forests comprised of saplings

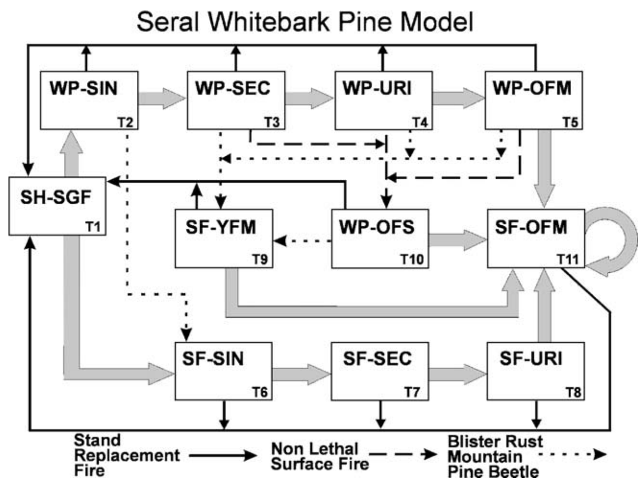

Fig. 1 – Successional pathways for a high elevation subalpine fir potential vegetation type as dictated by a successional model (Keane et al., 2002a). Cover types are shrub/herb (SH), whitebark pine (WP), subapline fir (SF). Structural stages are stand initiation (SIN), shrub/grass/forb (SGF), stem exclusion closed (SEC), understory re-initiation (URI), old forest multi-strata (OFM), old forest single strata (OFS), and young forest multi-strata (YFM).

and poles may be set back to grass and shrub communities by low intensity fire. Recognition of the prevalence of multiple successional pathways implies in a natural ecosystem, the distribution of successional classes is within the historical range of variation (Keane et al., 2002a; Landres et al., 1999). Before proceeding further, it is convenient to establish notation and terminology.

1.2. *Notation and terminology*

Let X_i denote a vector those elements are the frequency of occurrence for p successional classes for some landscape unit at time i . There are n such vectors sampled from a simulation of historical conditions, and these are indexed by $i = 1, \ldots, n$. The vector X_0 is an observation on the current successional class distribution. In this article, a landscape unit is comprised of 900, 30 m × 30 m pixels, each of which belongs to a single successional class at time i . Consequently, the successional class vector X_i consists of the number of pixels in each of the successional classes, subject to the constraint $\sum_j X_{ij} = 900$. The data, historical and current, are collected as an $n + 1 \times p$ matrix

$$\mathbf{X} = \begin{pmatrix} X_0^{\mathrm{T}} \\ X_1^{\mathrm{T}} \\ \vdots \\ X_n^{\mathrm{T}} \end{pmatrix},$$

where X_i^{T} denotes the transpose of X_i. The i, jth element of $\mathbf{X}$ is denoted by x_{ij}. The jth column mean is denoted by $\bar{x}_{\cdot j} = n^{-1} \sum_{i=1}^{n} x_{ij}$, and the p-vector of column means is $\bar{X} = (\bar{x}_{\cdot 1}, \ldots, \bar{x}_{\cdot p})$. The $\mathcal{L}^2$ norm of the vector X is $\|X\|_2 = \sqrt{X^{\mathrm{T}}X}$. The $p \times p$ sample variance matrix is $\mathbf{D}$, and its spectral decomposition is $\mathbf{D} = \mathbf{V}\boldsymbol{\Lambda}\mathbf{V}^{\mathrm{T}}$, where $\boldsymbol{\Lambda} = \mathrm{diag}(\lambda_1, \lambda_2, \ldots, \lambda_p)$ is a diagonal matrix comprised of the eigenvalues of $\mathbf{D}$ with the eigenvalues arranged in descending order, i.e., $\lambda_1 \geq \lambda_2 \geq \cdots \geq \lambda_p$ (Healy, 1986, Chapter 7). The matrix $\mathbf{V} = (V_1, V_2, \ldots, V_p)$ is comprised of the normalized eigenvectors of $\mathbf{D}$ arranged in concordance with the ordering on the eigenvalues. For the problem at hand, $\mathbf{X}$ is not full rank and $\mathbf{D}$ is singular because there are multiple constraints on the columns of $\mathbf{X}$. Suppose that the rank of $\mathbf{X}$ is $r \leq \min(n + 1, p)$. Let $\boldsymbol{\Lambda}_r$ denote the square submatrix of $\boldsymbol{\Lambda}$ containing the r positive eigenvalues and $\mathbf{V}_r = (V_1, \ldots, V_r)$ denote the submatrix of $\mathbf{V}$ corresponding to the positive eigenvalues. The Moore–Penrose generalized inverse of $\mathbf{D}$ is

$$\mathbf{D}^{-} = \mathbf{V}_r \boldsymbol{\Lambda}_r^{-1} \mathbf{V}_r^{\mathrm{T}}$$

(Healy, 1986, Chapter 5; Schott, 1997, Chapter 5). Because $\lambda_i > 0$ for $i = 1, \ldots, r$, $\mathbf{D}^{-}$ is positive definite and can be used to define a vector norm $\|X_0\|_{\mathbf{D}^{-}} = \sqrt{X_0^{\mathrm{T}}\mathbf{D}^{-}X_0} = \|\boldsymbol{\Lambda}_r^{-1/2}\mathbf{V}_r^{\mathrm{T}}X_0\|_2$, where $\boldsymbol{\Lambda}_r^{-1/2}$ is the diagonal matrix with diagonal elements $\lambda_i^{-1/2}$, and a distance function $\rho(X, Y) = \|X - Y\|_{\mathbf{D}^{-}}$. Finally, the matrix constructed by removing the ith row, or observation, from x is denoted by $\mathbf{X}_i$.

2. Methodology

The methodology for assessing the departure of a landscape unit from historical conditions consists of two stages, (1) generating a sample of observations on the distribution of successional classes by simulating succession under historical fire regimes, and (2) comparing the observed (current) successional class distribution to the simulated historical data.

2.1. *Simulating plant community succession*

The LANDscape SUccession Model (LANDSUM) (Keane et al., 2002a, 2006) was used to generate observations on successional class distribution. The predecessor of LANDSUM is CRBSUM, a model used to simulate coarse scale vegetation dynamics in the interior Columbia River Basin at a 1 km lattice cell resolution (Keane et al., 1996). Unlike CRBSUM, the LANDSUM model is spatially explicit. Simulations are carried out on a 30 m × 30 m pixel lattice covering a region of interest, typically 100–10,000 km^2 in area. A geographic information system maintains the lattice and stores attribute values on topography, potential vegetation type and prevailing wind direction for each pixel in addition to successional class. From an initial state, time is simultaneously incremented for all pixels. As time advances, a time series of successional classes is generated for each pixel in response to succession and fire disturbance. Successional transition between classes occurs at predetermined time intervals along potential vegetation type-specific successional pathways. In contrast to the deterministic progression of succession, fire disturbance is stochastic, and fires are generated according to potential vegetation type-specific annual ignition probabilities. Fire is spread from pixel to pixel as a function of prevailing wind direction and speed, and slope (Keane et al., 2002a; Rothermel, 1991). Fire events change the successional pathway according to fire intensity (low, medium or high intensity) as specified by the potential vegetation type successional model (Keane et al., 1996).

A simulation is carried out for a core region (the area of interest) by enlarging the simulation region to include a perimeter region. The perimeter allows for the spread of fires into the core region from outside. Potential vegetation type and current successional class are determined by field observation or by a classification rule that uses remote sensing variables for prediction of each pixel in a simulation region. The initial succession class for each pixel is defined to be the modal succession class under current conditions for the pixel's previously identified potential vegetation type. Time is incremented in 1-year steps for 5000 years. Output from the first 500 years of the simulation are discarded, and data from the remaining years are sampled every 20 years for the analysis of departure. This initialization strategy was adopted after conducting a pilot study using a sample of 266 landscape units. Simulations were carried out for 10,000 years, data were collected on a 10 year interval, and the departures of each historical sample year from all other historical sample years were computed. The first years of the simulation produced large departure values which then declined steadily to a base level. Once this level was reached, departure varied randomly with no trend, and so the departure series appeared stationary, that is, without trend and unaffected by endogenous or exogenous disturbances. We concluded that the transition from the initial state to stationarity was complete after 400 years as there was no statistical evidence of low-order polynomial trend in the historical departure series after 400 years. Using this scheme, stochastic variation attributable to dynamic modeling of succession has little effect on the distribution of simulated successional classes and departure assessment. Furthermore, restarting the simulations with a different set of initial conditions and random seeds does not lead to two or more simulated historical sequences that lead to different inferences regarding departure.

With respect to serial correlation, a 50-year sampling interval appeared to be sufficient for producing a set of departure values free of serial correlation. Presently, the computational effort demanded by a 50-year sampling interval can be very costly for large-area problems, and shorter intervals (usually 20 years) are sometimes used despite the risk of generating serially correlated simulation output. Below, we discuss the interpretation of departure given that autocorrelation among the simulated historical observations cannot be ruled out.

Though the simulations are conducted using the secondary pixel lattice, the comparison of current and historical conditions is conducted using the coarser primary lattice comprised of landscape units. The primary lattice size (30 × 30 pixels) was chosen as it is appropriate for management decision-making. At this scale, and in landscapes with spatially variable topography such as the Rocky Mountains and intermountain West, historical successional class distributions are substantially different among adjacent landscape units. Departure is computed for each landscape unit without considering neighboring landscape units because inference is primarily centered on comparing historical and current conditions in each landscape unit rather than larger geographic areas. For this reason, spatial correlation has been ignored.

Scale and resolution limitations affect LANDSUM simulations for a number of reasons. Recent simulation experiments have shown that the size of the landscape has a large influence on variation in the simulated successional process (Karau and Keane, submitted for publication). Small landscapes ($<10\,\mathrm{km}^2$) lead to greater variation in the simulated successional processes due to the scale at which fires are spread across the landscape. Specifically, fires are more likely to affect a large proportion of landscape and thereby perturb the landscape to a greater extent than fires in large landscapes. In contrast, Karau and Keane (submitted for publication) found that pixel size had little effect on simulated successional processes provided that pixel size was no greater than $300\,\mathrm{m} \times 300\,\mathrm{m}$. The coarseness of the successional classification system (as quantified by the number of potential vegetation type/successional class combinations) also influences the variability of the simulated successional process. In particular, less successional process variability was observed in those landscapes modeled with fewer classes (Karau and Keane, submitted for publication).

2.2. *Comparing observed and simulated plant community distributions*

In general terms, the objective is to determine whether an observation X_0 describing the current, or existing distribution of successional classes for a landscape unit is unusual with respect to the stochastic process that generated the observation vectors X_i, $i = 1, \ldots, n$, on historical conditions. We adopt the null hypothesis view, and proceed by assuming that X_0 was generated by the historical succession process. As discussed above, $\mathbf{X}$ is comprised of the $n + 1$ row vectors (including X_0^{T}), and the row vectors consist of the counts of pixels belonging to each combination of potential vegetation type and successional class at a point in time. The dimension of $\mathbf{X}$ is $n + 1 \times p$, and it is not unusual for p to be larger than n; for example, a random sample of 5628 landscape units from a pilot region discussed below produced median value of p of 175, and the 5th and 95th percentiles of p were 96 and 231, respectively. A column constraint is imposed on $\mathbf{X}$ by the condition that the number of pixels (and hence, the row totals) are fixed at 900 for each year. Each potential vegetation type observed on the landscape unit induces an additional linear constraint on the columns of $\mathbf{X}$ because the pixel count within potential vegetation type is also fixed across years.

There are similarities between this problem and two-sample and multivariate outlier detection problems. With respect to the two-sample approach, it is useful to view the data as a $2 \times p$ contingency table obtained by cross-classifying data source (historical and current) versus potential vegetation type/successional class pair. A test of departure is obtained, in principle, by the Chi-square test of homogeneity of proportions. However, the majority of the expected cell counts for current conditions are typically less than one because of the tendency for a few successional classes to dominate the count distributions. It is inappropriate, then, to model the data using the multinomial distribution and to assess departure by conducting a Chi-square test of homogeneity of proportions. In addition, the cell counts on historical conditions are totals obtained over multiple years, and these counts are sometimes correlated.

Assessing departure is similar to identifying multivariate outliers as both tasks attempt to identify unusual observations by comparing a candidate observation to a set of observations. Multivariate outlier detection methods tend to be largely distribution-free and suited for high-dimensional data, characteristics that are also desirable for departure assessment. Traditional multivariate outlier detection methods identify observations that are distant from a measure of central tendency such as the sample mean. Mahalanobis distance, the simplest and arguably the most commonly used multivariate outlier detection measure is $d_M(X_0) = \sqrt{(X_0 - \bar{X})^T \mathbf{D}^{-1}(X_0 - \bar{X})}$ where $\mathbf{D}$ is the full rank sample variance matrix. When $\mathbf{D}$ is not full rank, then an analogous distance measure is $d_M^r(X_0) = \|\mathbf{\Lambda}_r^{-1/2}\mathbf{V}_r(X_0 - \bar{X})\|_2$. The distance measure d_M^r gives equal weight to each eigenvector axis in the sense that the vector $V = \mathbf{\Lambda}_r^{-1/2}\mathbf{V}_r(X_0 - \bar{X})$ satisfies $\mathrm{var}(V) = \mathbf{I}$ provided that $\mathrm{var}(X_0) = \mathbf{D}$. Multivariate outlier detection distance measures are often based on the spectral decomposition of the sample variance matrix $\mathbf{D}$ (see Jolliffe (2002), Chapter 10). For example, Gnanadesikhan and Kettenring (1972) consider a distance measure that emphasizes variables with larger sample variances. When $\mathbf{D}$ is not full rank, then the measure can be expressed as $d_{GK}^r(X_0) = \|\mathbf{\Lambda}_r^{1/2}\mathbf{V}_r(X_0 - \bar{X})\|_2$. Observations that are distant with respect to d_M and d_{GK} tend to be outliers respect to one or more of the column variables comprising $\mathbf{X}$, and so are often detectable by univariate methods provided that p is not very large. Consequently, other distance measures attempt to expose observations that are unusual in some respect that is not obvious using univariate methods (Jolliffe, 2002, Chapter 10). For example, these measure may place greater weight on those eigenvectors with the least contribution towards explaining variation in $\mathbf{X}$. Two examples are $d_1^s(X_0) = \|\mathbf{V}_s(X_0 - \bar{X})\|_2$ and $d_2^s(X_0) = \|\mathbf{\Lambda}_s^{-1/2}\mathbf{V}_s(X_0 - \bar{X})\|_2$, where $\mathbf{V}_s$ denotes a matrix constructed from those eigenvectors of $\mathbf{D}$ corresponding to the s smallest positive eigenvalues (Jolliffe, 2002, Chapter 10). A complication associated these measures is that it is sometimes difficult to discriminate between very small positive eigenvalues and zero-valued eigenvalues when p is large (say, $p > 30$).

These traditional multivariate outlier detection approaches are not necessarily well-suited for detecting departure of current from historical conditions. Specifically, the successional process may generate several common patterns of successional class distributions, or modes, and measuring distance to a single centroid such as $\bar{X}$ may mistakenly identify observations as outliers that are near a mode, but not the centroid. In addition, the appropriate number of eigenvector axes with which to measure distance varies among landscape units, and it is impractical to determine appropriate axes when there are many landscape units in the region of interest. More recent outlier detection methods focus on robustness against swamping, or maintaining sensitivity when many outliers are present. Jackson and Chen (2004), Juan and Prieto (2001), Pena and Preito (2001), Penny and Jolliffe (2001) provide examples. These methods are computationally intensive, and not appropriate for this application in which departure must be evaluated for thousands of landscape units; moreover, swamping is not a concern because the simulated historic data is free of observational error.

2.3. *The projection method of assessing departure*

We propose an approach to assessing departure based the extent to which a suspected outlier X_0 can be approximated as a linear combination of all other observations in the data set. This is accomplished by projecting the vector X_0 onto the space spanned by the rows of $\mathbf{X}_0$, where $\mathbf{X}_0$ is obtained by deleting the row vector X_0^T from $\mathbf{X}$. We propose using the scaled length of the residual error vector to measure the departure of X_0 from the distribution that generated the rows of $\mathbf{X}_0$. Let $\mathbf{P}$ denote a projection matrix for $\mathcal{R}(\mathbf{X}_0)$, the linear subspace of $\mathbb{R}^p$ spanned by the rows of $\mathbf{X}_0$. If $\mathbf{X}_0\mathbf{X}_0^T$ is nonsingular, then

$$\underset{p\times p}{\mathbf{P}} = \mathbf{X}_0^T(\mathbf{X}_0\mathbf{X}_0^T)^{-1}\mathbf{X}_0, \tag{1}$$

and the projection of X_0 onto $\mathcal{R}(\mathbf{X}_0)$ is $U = \mathbf{P}X_0$. If $\mathbf{X}_0\mathbf{X}_0^T$ is singular, and $(\mathbf{X}_0\mathbf{X}_0^T)^-$ is any generalized inverse of $\mathbf{X}_0\mathbf{X}_0^T$, then $\mathbf{P} = \mathbf{X}_0^T(\mathbf{X}_0\mathbf{X}_0^T)^-\mathbf{X}_0$ is the unique projection matrix for $\mathcal{R}(\mathbf{X}_0)$. A projection matrix for $\mathcal{R}(\mathbf{X}_0)^\perp$, the null space of $\mathcal{R}(\mathbf{X}_0)$, is $\mathbf{I}_p - \mathbf{P}$. The projection of a conformable vector X onto $\mathcal{R}(\mathbf{X})^\perp$ is $V = (\mathbf{I}_p - \mathbf{P})X$ (Schott, 1997, Chapter 2). The vector V is often called the residual or error vector associated with the projection U because $X - U = V$. Our measure of the distance between X and $\mathbf{X}_0$ is the scaled length of the error vector given by

$$d_P(X, \mathbf{X}_0) = \frac{\|(\mathbf{I}_p - \mathbf{P})X\|_2}{\|X\|_2}.$$

This distance may also be viewed as the length of the error vector obtained by projecting the normalized vector $X/\|X\|_2$ onto $\mathcal{R}(\mathbf{X}_0)^\perp$. It is readily verified that the length of the error vector $V = (\mathbf{I}_p - \mathbf{P})X$ is no greater than the length of X, and hence, $0 \le d_P(X, \mathbf{X}_0) \le 1$. In addition, the projection $U = \mathbf{P}X$ is the least squares prediction of X obtained by regressing X on the rows of $\mathbf{X}_0$.

Returning to the problem of assessing departure of the current data vector X_0, the $n \times n$ matrix $\mathbf{X}_0\mathbf{X}_0^T$ is not full rank, and formula (1) cannot be used to compute the projection matrix. Appendix A shows that a relatively simple method of computing $d_P(X_0, \mathbf{X}_0)$ can be carried out by extracting the eigenvectors of $\mathbf{X}_0^T\mathbf{X}_0$. Specifically, suppose that the $p \times r$ matrix $\mathbf{U}_r = (U_1, \ldots, U_r)$ is comprised of the r eigenvectors of $\mathbf{X}_0^T\mathbf{X}_0$ corresponding to the $r \le p$ positive eigenvalues of $\mathbf{X}_0^T\mathbf{X}_0$. Then, as shown in Appendix A, the departure of X_0 from $\mathbf{X}_0$ is

$$d_P(X_0, \mathbf{X}_0) = \frac{\|(\mathbf{I}_p - \mathbf{U}_r\mathbf{U}_r^T)X_0\|_2}{\|X_0\|_2} = 1 - \frac{\|\mathbf{U}_r\mathbf{U}_r^T X_0\|_2}{\|X_0\|_2}.$$

This formula is preferable to formula (1) from a computational standpoint because it is not necessary to compute $\mathbf{P}$. Consequently, the singularity $\mathbf{X}_0\mathbf{X}_0^T$ is not a concern.

The primary difference between the projection method and conventional outlier detection methods is that the projection method does not center the data matrix $\mathbf{X}$ or the test vector X_0, whereas the conventional measures center both. By centering $\mathbf{X}$, distances are measured along the eigenvectors of the sample variance matrix $\mathbf{D} = n^{-1}(X - \mathbf{1}\bar{X}^{\mathrm{T}})^{\mathrm{T}}(X - \mathbf{1}\bar{X}^{\mathrm{T}}) = n^{-1}\mathbf{X}^{\mathrm{T}}\mathbf{X} - \bar{X}\bar{X}^{\mathrm{T}}$ where $\mathbf{1}$ is an vector of ones. The conventional outlier detection methods differ with respect to the relative importance of the eigenvectors towards the distance calculation. For example, successional classes (columns of $\mathbf{X}$) with large variability are of diminished importance in determining Mahalanobis distance (d_{M}), and of greater importance for d_{GK}. Let $\bar{X}_0 = n^{-1}\mathbf{X}_0^{\mathrm{T}}\mathbf{1}$. In contrast to d_{M}, the projection method distance d measures distance along the eigenvectors of $\mathbf{X}_0^{\mathrm{T}}\mathbf{X}_0 = n(\mathbf{D}_0 + \bar{X}_0\bar{X}_0^{\mathrm{T}})$, and consequently, the importance of the eigenvector axes associated with d are determined by the sample mean vector $\bar{X}_0 = n^{-1}\mathbf{X}_0\mathbf{1}$ and the sample variance matrix $\mathbf{D}_0$, both constructed without X_0. In addition, the projection of a vector X onto these eigenvector axes strongly reflects the magnitude of the different successional class counts whereas the conventional measures project the centered vector $X - \bar{X}$ onto the eigenvector axes of $\mathbf{D}$ which poorly reflects the magnitude of different successional classes. Our strategy of projecting X_0 without centering is preferable if the successional process generates several modes so that the sample mean is not effective for describing the population of successional class vectors.

2.4. *Significance testing*

In this section, a permutation procedure (Good, 1993) is described for testing $H_0 : X_0 \in \mathcal{S}$ versus $H_1 : X_0 \notin \mathcal{S}$ assuming $X_0, X_1, \ldots, X_n$ are mutually independent, where $\mathcal{S}$ denotes the historical population of successional class vectors. Let D_{P} denote the statistic generating the observed departure $d_{\mathrm{P}}(X_0, \mathbf{X}_0)$. Under H_0, $X_0, X_1, \ldots, X_n$ are independent observations sampled from $\mathcal{S}$, and the empirical distribution of D_{P} is obtained by enumerating all possible values of $d_{\mathrm{P}}(X_k, \mathbf{X}_k)$, $k = 0, 1, \ldots, n$. This entails constructing all $n+1$ partitions of $\mathbf{X}$ that consist of a singleton set $\{X_k\}$ and $\mathbf{X}_k$, and computing the departure of X_k from $\mathbf{X}_k$. The test statistic, N_+, is number of values $d_{\mathrm{P}}(X_k, \mathbf{X}_k)$, $k = 0, 1, \ldots, n$, that are greater than or equal to the observed departure $d_{\mathrm{P}}(X_0, \mathbf{X}_0)$, and the observed significance level is $N_+/(n+1)$. An appropriate use of this test is to measure the strength of evidence of departure for comparative purposes rather than formal testing. Two reasons argue against formal hypothesis testing. First, departure analysis is typically carried out simultaneously for many landscape units comprising a region of interest, and some provision for controlling experiment-wise Type I error rates should be available. The application of these methods is complicated by possible spatial correlation among landscape units that are close in space, and tend to be similar with respect to vegetation and fire history. In addition, the possibility of serial correlation among $X_1, \ldots, X_n$ implies that observed significance levels may be inflated or deflated relative to observed significance levels obtained from serially uncorrelated historical data. For simplicity, we refer to $N_+/(n+1)$ as the observed significance level with the warning that significance testing is not advisable unless the problems of serial and spatial correlation are carefully considered.

One concern raised regarding the proposed departure measure is whether departure is dependent on successional class complexity. In other words, can similar inferences be drawn from a particular value of departure regardless of the number of successional classes present in the historical data? The observed significance level obtained from the permutation test is comparable across landscape units because it is the proportion of null distribution departures that are as large as the observed departure. There is however, some support for the comparability of $d_{\mathrm{P}}(X_0, \mathbf{X}_0)$ across landscape units in a sample of 5628 landscape units drawn from the 76,924 landscape units comprising the Utah pilot region. The analysis of these data, described below, shows that departure and observed significance level are strongly associated. Thus, a departure value that is unusually large in one landscape unit, and hence, associated with a small observed significance level, will also tend to be associated with similar small observed significance levels in other landscape units.

3. An example

Lands administered by the USDA Forest Service in Utah (Zone 16 in the Forest Service Nationwide Map) are one of two pilot areas used to develop and test the methodology. This region consists of N =76,924 landscape units. The predominant vegetation of the region is montane conifer forest, though there are extensive grass and shrublands, and some subalpine forest. Alpine communities are present but lesser in area. Fire suppression was vigorously pursued in this region during the last century; in addition, overgrazing has led to the establishment of invasive species in many grassland and shrubland locations. Long et al. (in press) provide an extensive description of the historical fire regimes used in the LANDSUM simulations. To provide a example of typical successional patterns in this area, a single landscape unit was randomly selected and the average percent areal cover over time of the 22 most common potential vegetation type/succession class combinations (out of 60) are listed in Table 1. Fig. 2 is a visual representation of the data matrix $\mathbf{X}$ from which Table 1 was constructed. This figure consists of 60×202 cells corresponding to 60 successional classes and $202 = 201 + 1$ years of data. The degree of shading for the i, jth each cell corresponds to the number of pixels occupied by successional class i in year j. At any point in time, the great majority of the 900 pixels to belong to only a few potential vegetation type/succession class combinations. Moreover, there are a few dominant potential vegetation type/succession class combinations that tend to dominate the pixel counts for extended intervals. The length of time during which these classes are dominant appears to vary substantially among these classes. For the remainder of the potential vegetation type/successional class combinations, usually few or no pixels belong to these combinations at any point in time. This pattern is characteristic of fire regimes in which low intensity fire serves to maintain stands in mid-successional communities by removing regeneration in the understory.

Departure for the Zone 16 pilot region is displayed as a gray-scale map (Fig. 3). The larger departure values primarily were observed in non-forest potential vegetation types (salt desert shrub and pinion-juniper types), probably because of overgrazing in these types and the consequent replacement of native forb and grass species by invasive species. Substantial departure was also detected in montane forest potential

Table 1 – List of the 22 potential vegetation type/successional class combinations with the largest areal covers under the simulated historical fire regime for the stratum displayed in Fig. 2

Potential vegetation type	Successional classes	Average areal cover (%)
White Fir/Maple	All classes	27.0
	Early seral	11.6
	Mid seral	6.7
	Late seral	3.2
	Mid seral disturbance maintained	1.9
Pinyon-Juniper/North	All classes	13.6
	Early seral herb	2.6
	Early seral shrub	1.6
	Mid seral shrub	2.6
	Late seral shrub	1.2
	Early seral grass	2.0
	Mid seral grass	1.5
Pinyon-Juniper/Sagebrush	All classes	5.7
	Early seral shrub	1.2
	Mid seral grass	1.6
Pinyon-Juniper/South	All classes	3.4
	Mid seral grass	1.2
Pinyon-Juniper/Mountain Mahogany	All classes	3.2
	Mid seral shrub	1.6
Mountain Big Sagebrush	All classes	22.1
	Early seral	5.4
	Mid seral shrub	2.7
	Mid seral shrub	1.3
	Late seral shrub	1.4
	Early seral grass	4.8
	mid seral grass	3.8
Riparian Hardwood	All classes	9.2
	Early seral	1.5
	Mid seral	1.8

vegetation types (such as Douglas-fir/Ponderosa pine) that historically were subject to frequent, low intensity fires.

A sample of 5628 landscape units were drawn from the population of 76,924 units to investigate the relationship between

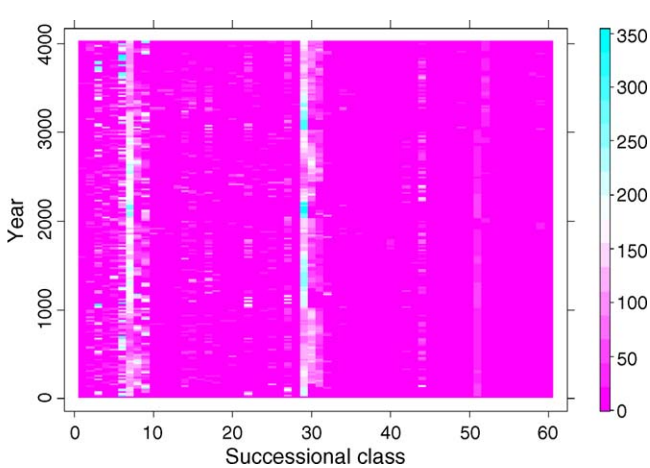

Fig. 2 – A level plot constructed for a stratum showing the numbers of observations in each potential vegetation type/succession class combination.

departure and observed significance level. On the natural logarithm scale, there is a strong linear correlation ($r = -0.74$) between departure and observed significance level based on 5498 observations with non-zero departure values. The transformed variables are visually displayed by aggregating departure according to observed significance level, and plotting box plots of log-departure against log-observed significance level (Fig. 4). A clear association is apparent between current year departure $d_P(X_0, \mathbf{X}_0)$ and observed significance as quantified by the fraction of historical departures that are greater than or equal to $d_P(X_0, \mathbf{X}_0)$. This implies consistency among landscape units with regard to the historical departure distributions, and that the scale on which departure is measured is roughly the same across the much of the pilot region.

4. A simulation study

A simulation study was carried out to compare the sensitivity of the departure measures discussed above. The simulation combined 201 observations sampled from the historic population of successional class vectors $\mathcal{S}$ and one or more atypical observations sampled from a different population, denoted by $\mathcal{S}_0$. Then, the departure of each observation in the combined sample was computed and classified as unusual, or not, depending on the departure value. An observation X_0 was classified as unusual if its departure value was larger than the 95th sample quantile of departure values. The sensitivity and specificity of a departure measure were determined from the proportion of observations sampled from $\mathcal{S}_0$ and $\mathcal{S}$, respectively, that were classified as unusual.

This simulation study is similar to those used in studies of outlier detection methods in that a set of atypical observations contaminates a sample, and the objective is to determine the accuracy with which the atypical observations are detected as unusual (and identified as outliers). An important property of outlier detection methods is resistance against swamping, or the ability to perform well when the contamination fraction is large. While resistance to swamping is not directly relevant to the comparison of current and historical conditions because there is only a single observation on current conditions, an analysis of resistance to swamping does provide some additional information on the projection method of departure assessment.

We randomly sampled five clusters of landscape units from Zone 16 for the simulation study. Successional processes were simulated for each cluster under historical fire regimes, and historical data were drawn from the core regions, and provided $5 \times 266 = 1330$ landscape units. For each unit, outliers were created by randomly sampling m observations with replacement from the historic sample of n observations, where m was a predetermined fraction of n. These m observations were made atypical by randomly permuting the succession class counts within each potential vegetation type. Specifically, suppose that the p-vector X consists of counts from s potential vegetation types, and that there are p_j succession classes in potential vegetation type $j, j = 1, \ldots, s$. Then X can be viewed as comprised of s sub-vectors, where the elements in the sub-vector X_j are the counts for each p_j succession class within potential vegetation type j. Atypical count vectors

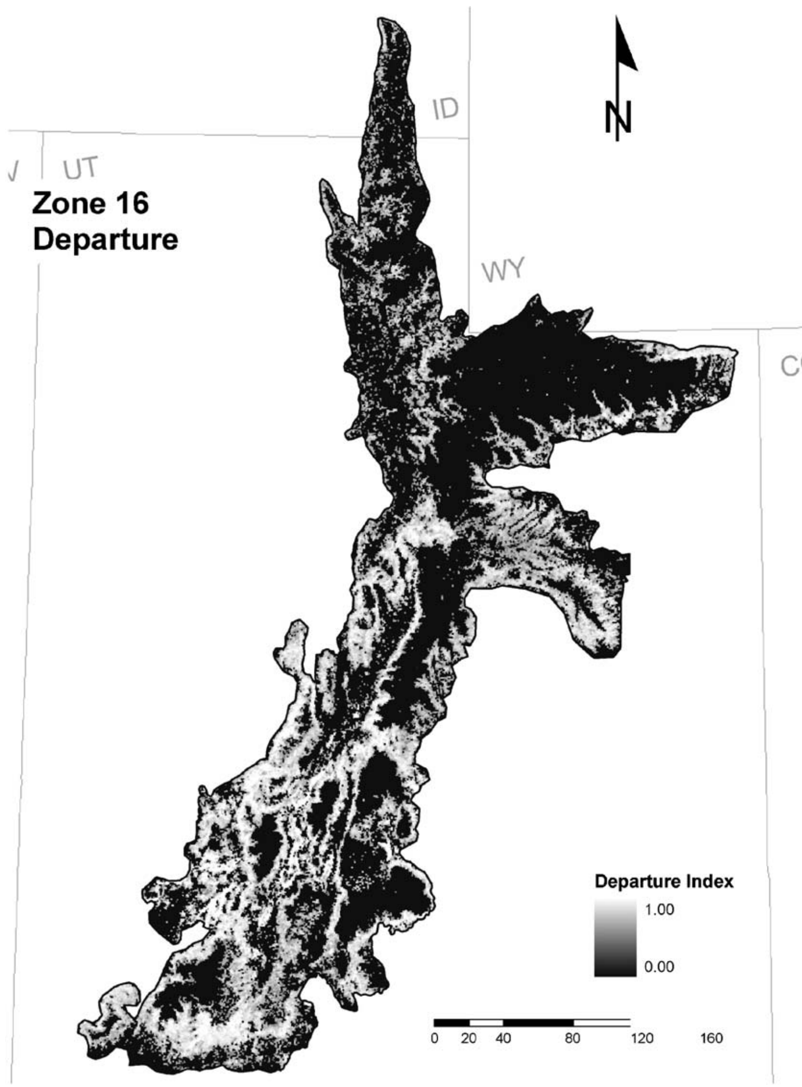

Fig. 3 – Gray-scale map of departure for the Utah pilot region constructed from 76,924 landscape units.

were generated by randomly permuting the elements of X_j for each $j = 1, \ldots, s$. Because counts were permuted only within potential vegetation type class, the permuted observations were subject to the same linear constraints as the original observations, and the rank of the combined data matrix was the same as the historical data set. At the same time, these additional contaminant observations are presumably inconsistent with the process that generated $\mathcal{S}$ because the counts have been permuted. Contaminant observations were introduced according to six rates: 1, 5, 10, 15, 20, and 25% of the historical data sample of $n = 201$ observations.

A second simulation scheme was used in which outliers were obtained by random sampling m observations from landscape units different than the one being analyzed. Consequently, the potential vegetation types represented in the contaminant observations were sometimes different than in the historical observations, and the rank of the combined data matrix tended to be greater than the historical data matrix. Results from the two schemes were not substantially different, so we report the results only for the first simulation scheme.

The outlier detection methods used in the simulation study differ with respect to the measurement of observation-to-set distance. The distance measures are the projection method distance d_{P}, Mahalanobis distance d_{M}^{r} (adapted for less-than-full rank covariance matrices), d_{GK}^{r} (Gnanadesikhan and Kettenring, 1972), and d_1^{s} and d_2^{s} (Jolliffe, 2002, Chapter 10). An observation X_k was identified as an outlier if the distance to the historical data set $\mathbf{X}_k$ was greater than the qth quantile of all such distances. Two values of q were used, 0.90 and 0.95. Because there was very little difference in the relative performance of the methods with respect to the two quantiles, we present results only for the 95th quantile. Two statistics were computed to compare methods: the detection rate, or sensitivity (percent of contaminants identified as outliers), and the specificity (percent of non-contaminants not identified as outliers). By using the 95th quantile as a criterion for outlier detection, 10 observations will be identified as outliers by each method. By fixing the number of identified outliers to be 10, specificity is forced to be less than 100% when the contamination fraction is less than 5%. For example, if the contamination

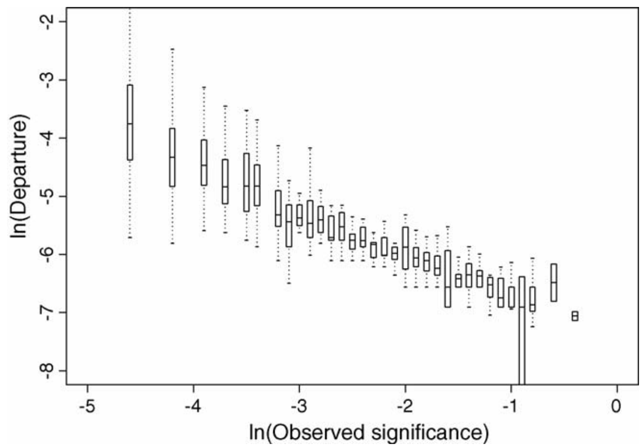

Fig. 4 – Box plots of log-departure plotted against log-observed significance level using a random sample of 5498 landscape units with non-zero departure values. Log-departure was aggregated according to the associated observed significance levels.

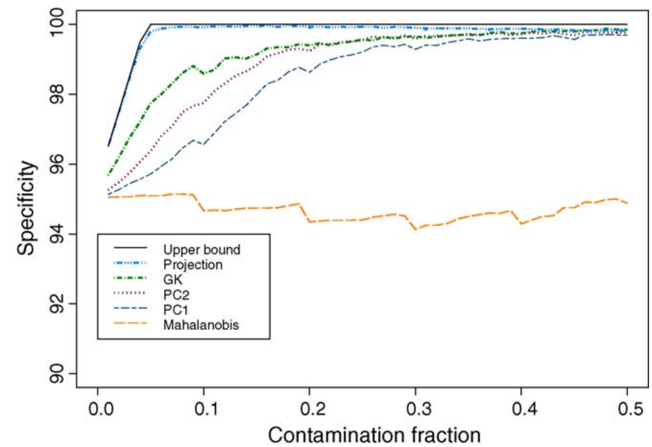

Fig. 6 – Specificity plotted against contamination fraction for five departure measures. Plotted values are means over 1330 landscape units. The departure measures are (1) d_P, denoted by projection in the legend, (2) d^r_{GK} (Gnanadesikhan and Kettenring, 1972), denoted by GK in the legend, (3) d^s_2, denoted by PC2 in the legend, (4) d^s_1, denoted by PC1 in the legend, and (5) d_M, Mahalanobis distance.

rate is 1%, then two of the 201 observations are contaminants; if these are correctly identified, then the detection rate is 100%. But, eight additional non-contaminants will be identified as outliers and the specificity will be $100 \times 191/199 = 96.0\%$. Similarly, the detection rate is bounded above by $100 \times 10/(201c)$, where c is the contamination fraction. When the contamination fraction is 0.1, then detection rate is bounded above by 50%.

Figs. 5 and 6 summarize the results of the simulation analysis. Fig. 5 shows that the detection rate is substantially greater for the projection method compared to the other methods, particularly when the fraction of contaminants was small (say, less than or equal to 0.01). In addition, Fig. 6 shows that the specificity was greatest for the projection method at all contamination rates. The performance of d_{GK} was best among the four conventional outlier distance measures, and most similar to d_P. This result is in concordance with the discussion of the distance measures above because the eigenvector axes for d_{GK} and d_P are extracted from matrices that give greater weight to successional classes with the largest sample variances.

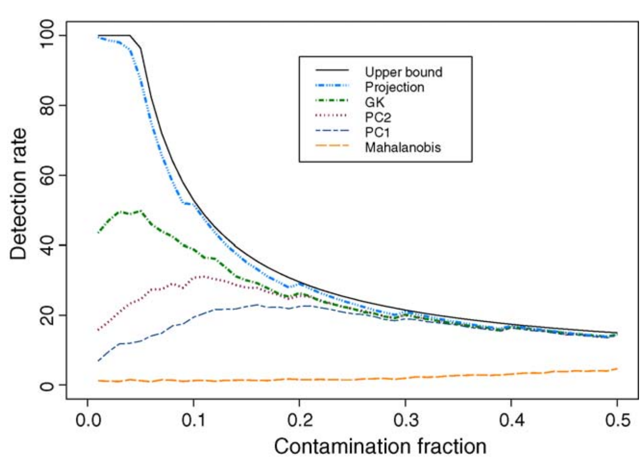

Fig. 5 – Outlier detection rate (sensitivity) plotted against contamination fraction for five departure measures. Plotted values are means over 1330 landscape units. The departure measures are (1) d_P, denoted by projection in the legend, (2) d^r_{GK} (Gnanadesikhan and Kettenring, 1972), denoted by GK in the legend, (3) d^s_2, denoted by PC2 in the legend, (4) d^s_1, denoted by PC1 in the legend, and (5) d_M, Mahalanobis distance.

5. Discussion

Simulated observations are less desirable than sample observations because simulated data depend on the assumptions of the model that generated the data. However, it is sometimes impossible to effectively sample ecological and environmental systems over time and space. Comparing current successional class distributions to historical distributions illustrates the problem because data on historical conditions (pre-European settlement) is very sparse. We conclude, based on this study, that simulations of successional processes are useful for comparative purposes. Specifically, these data are appropriate for assessing relative departure across contiguous regions, and thereby identifying areas and plant community types where current distribution of successional classes appears to have diverged from historical conditions. Given the limitations associated with simulated data, the appropriate use of the methodology discussed herein is for prioritizing landscape units for field visitation and possible treatment. Our recommendation to land managers is to use a two-stage procedure. In the first stage, a subset of all landscape units within a region with large departure values and small observed significance levels should be identified. The second stage is ground visitation and inspection, and a final determination of management activities.

The methodology presented in this article incorporates two important features. First, the simulation of successional processes is spatially explicit. Incorporating the spatial dimension has a significant impact on the simulation of fire disturbance events. In contrast, previous simulators of succession modeled each map unit independently, without consideration of fire spread and the factors that influence it. While these programs may faithfully simulate fire disturbance on average, accuracy for individual map units may be poor in landscapes with high relief because fire intensity and spread, and hence frequency, is partly governed by topography and wind direction.

The second important feature is the use of the projection method as a distance measure for comparing a single observation to a set of observations on historical conditions. This distance measure differs from traditional outlier detection methods that measure distance between X_0 and the centroid $\bar{X}$ along particular eigenvector axes extracted from the sample variance matrix. The projection method constructs a prediction of X_0 that is a linear combination of the historic data vectors, and measures the prediction error. The prediction error is determined by the extent to which the distribution of counts across successional classes in the test vector can be approximated by the historical observation vectors. The simulation study indicates that the projection method measure of departure is substantially more sensitive than the comparison outlier detection methods. We attribute this sensitivity primarily to using un-centered test vectors in the distance calculation, and to a lesser extent, measuring distance along the eigenvectors of $\mathbf{X}_0^{\mathrm{T}}\mathbf{X}_0$. The eigenvectors $\mathbf{X}_0^{\mathrm{T}}\mathbf{X}_0$ and $\mathbf{D}_0$ are often not substantially different; on the other hand, X_0 and $X_0 - \bar{X}_0$ are always very different, and so we surmise that not centering X_0 is important for sensitivity. Moreover, we conclude the difference in performance between the comparison outlier detection methods and the projection method is attributable to historical data that are a mixture of successional class distributions without a clear mode.

Acknowledgements

This project was funded by the USDA Forest Service Rocky Mountain Research Station Missoula Fire Sciences Laboratory (03-JV-11222048-151) and USDA Forest Service Fire and Aviation Management (FAM) LANDFIRE prototype project. We thank Sarah Pratt and Lisa Holsinger USDA Forest Service Rocky Mountain Research Station Missoula Fire Sciences Laboratory for their assistance with data and graphics, and two anonymous reviewers for helpful comments.

Appendix A. An alternate expression for departure

The singular value decomposition of $\mathbf{X}^{\mathrm{T}}$ provides a computationally convenient alternative to formula (1) for computing departure. To develop the alternative formula, let $\gamma_i, i = 1, \ldots, n$ denote the eigenvalues of $\mathbf{XX}^{\mathrm{T}}$ arranged in descending order, $\mathbf{\Gamma}_p$ denote a diagonal matrix with diagonal elements $\sqrt{\gamma_i}$, and $\mathbf{\Gamma}$ a $p \times n$ matrix

$$\mathbf{\Gamma} = \begin{pmatrix} \underset{p\times p}{\mathbf{\Gamma}_p} & \underset{p\times n-p}{\mathbf{0}} \end{pmatrix},$$

where $\mathbf{0}$ denotes a matrix of zeros. The singular value decomposition of the $p \times n$ matrix $\mathbf{X}^{\mathrm{T}}$ can be expressed as $\mathbf{X}^{\mathrm{T}} = \mathbf{U\Gamma V}^{\mathrm{T}}$, where $\underset{p\times p}{\mathbf{U}}$ and $\underset{n\times n}{\mathbf{V}}$ are comprised of the eigenvectors of $\mathbf{X}^{\mathrm{T}}\mathbf{X}$ and $\mathbf{XX}^{\mathrm{T}}$, respectively. Suppose that the rank of $\mathbf{X}^{\mathrm{T}}$ is $r \leq \min(n+1, p)$ and $\mathbf{\Gamma}_r$ denotes the square submatrix of $\mathbf{\Gamma}_p$ containing the r square roots of the positive eigenvalues of $\mathbf{X}^{\mathrm{T}}\mathbf{X}$ (Schott, 1997, Chapter 4). The truncated singular value decomposition of $\mathbf{X}^{\mathrm{T}}$ is obtained by partitioning $\mathbf{U}$ and $\mathbf{V}^{\mathrm{T}}$ conformably with $\mathbf{\Gamma}_r$ according to

$$\mathbf{X}^{\mathrm{T}} = \begin{pmatrix} \underset{p\times r}{\mathbf{U}_r} & \underset{p\times p-r}{\mathbf{U}_{p-r}} \end{pmatrix} \begin{pmatrix} \underset{r\times r}{\mathbf{\Gamma}_r} & \underset{r\times n-r}{\mathbf{0}} \\ \underset{p-r\times r}{\mathbf{0}} & \underset{p-r\times n-r}{\mathbf{0}} \end{pmatrix} \begin{pmatrix} \underset{n\times r}{\mathbf{V}_r^{\mathrm{T}}} & \underset{n\times n-r}{\mathbf{V}_{n-r}^{\mathrm{T}}} \end{pmatrix} = \mathbf{U}_r\mathbf{\Gamma}_r\mathbf{V}_r^{\mathrm{T}},$$

(Vogel, 2002, Chapter 1). A generalized inverse of $\mathbf{XX}^{\mathrm{T}}$ is $(\mathbf{XX}^{\mathrm{T}})^{-} = \mathbf{V}_r\mathbf{\Gamma}_r^{-2}\mathbf{V}_r^{\mathrm{T}}$, where $\mathbf{\Gamma}_r^{-2}$ is defined to be the diagonal matrix with diagonal elements γ_i^{-2}, $i = 1, \ldots, r$. Substituting $\mathbf{U}_r\mathbf{\Gamma}_r\mathbf{V}_r^{\mathrm{T}}$ for $\mathbf{X}^{\mathrm{T}}$ and $\mathbf{V}_r\mathbf{\Gamma}_r^{-2}\mathbf{V}_r^{\mathrm{T}}$ for $(\mathbf{XX}^{\mathrm{T}})^{-1}$ in formula (1) leads to

$$\mathbf{U}_r\mathbf{\Gamma}_r\mathbf{V}_r^{\mathrm{T}}\mathbf{V}_r\mathbf{\Gamma}_r^{-2}\mathbf{V}_r^{\mathrm{T}}\mathbf{V}_r\mathbf{\Gamma}_r\mathbf{U}_r^{\mathrm{T}} = \mathbf{U}_r\mathbf{U}_r^{\mathrm{T}}.$$

It is straightforward to verify that $\mathbf{U}_r\mathbf{U}_r^{\mathrm{T}}$ and $\mathbf{I}_p - \mathbf{U}_r\mathbf{U}_r^{\mathrm{T}}$ are projection matrices for the row and null space of $\mathbf{X}^{\mathrm{T}}$, respectively.

REFERENCES

Anderson, M., Bourgeron, P., Bryer, M.T., Crawford, R., Engelking, L., Faber-Langendoen, D., Gallyoun, M., Goodin, K., Grossman, D.H., Landaal, S., Metzler, K., Patterson, K.D., Pyne, M., Reid, M., Sneddon, L., Weakley, A.S., 1998. International classification of ecological communities: terrestrial vegetation of the United States, Volume II. The National Vegetation Classification System: List of Types. The Nature Conservancy, Arlington, Virginia, USA.

Arno, S.F., Parsons, D.J., Keane, R.E., 2000. Mixed-severity fire regimes in the northern Rocky Mountains: consequences of fire exclusion and options for the future. Wilderness Science in a Time of Change Conference, Volume 5: Wilderness Ecosystems, Threat, and Management. USDA Forest Service, Rocky Mountain Research Station, Fort Collins, CO.

Bettinger, P., Lennette, M., Johnson, K.N., Spies, T.A., 2004. A hierarchical spatial framework for forest landscape planning. Ecol. Model. 182, 25–48.

Botkin, D.B., Schenk, H.J., 1996. Review and analysis of JABOWA and related forest models and their use in climate change studies. NCASI Technical Bulletin Number 717.

Daubenmire, R., 1966. Vegetation: identification of typal communities. Science 151, 291–298.

DeBano, L.F., Neary, D.G., Ffolliott, P.F., 1998. Fire's Effect on Ecosystems. Wiley, New York.

Ferry, G.W., Clark, R.G., Montgomery, R.E., Mutch, R.W., Leenhouts, W.P., Zimmerman, G.T., 1995. Altered Fire Regimes Within Fire-adapted Ecosystems. USDI, National Biological Service, Washington, DC.

Frost, C.C., 1998. Presettlement fire frequency regimes of the United States: a first approximation. Tall Timbers Fire Ecol. Conf. 20, 70–81.
Gnanadesikhan, R., Kettenring, J.R., 1972. Robust estimates, residuals, and outlier detection with multiresponse data. Biometrics 28, 81–124.
GAO, 2002. Severe wildland fires: leadership and accountability needed to reduce risks to communities and resources. Report to Congressional Requesters GAO-02–259. US General Accounting Office, Washington, DC.
Good, P., 1993. Permutation Tests. Springer-Verlag, New York.
Grossman, D.H., Faber-Langendoen, D., Weakley, A.S., Anderson, M., Bourgeron, P., Crawford, R., Goodin, K., Landaal, S., Metzler, K., Patterson, K., Pyne, M., Reid, M., Sneddon, L., 1998. International classification of ecological communities: terrestrial vegetation of the United States, Volume I. The National Vegetation Classification System: Development, Status, and Applications. The Nature Conservancy, Arlington VA, USA.
Hann, W.J., Jones, J.L., Keane, R.E., Hessburg, P.F., Gravenmier, R.A., 1998. Landscape dynamics. J. Forest. 96, 10–15.
Healy, M.J.R., 1986. Matrices for Statistics. Clarendon Press, Oxford, UK.
Heinselman, M.L., 1981. Fire and succession in the conifer forests of North America. In: West, D.C., Shugart, H.H., Botkin, D.B. (Eds.), Forest Succession: Concepts and Applications. Springer-Verlag, New York, pp. 374–406.
Hessburg, P.F., Smith, B.G., Salter, R.B., 1999. Detecting change in forest spatial patterns from reference conditions. Ecol. Appl. 9, 1232–1252.
Jackson, D.A., Chen, Y., 2004. Robust principal component analysis and outlier detection with ecological data. Environmetrics 15, 129–139.
Jiang, H., Appsa, M.A., Zhanga, Y., Penga, C., Woodward, P.M., 1999. Modeling the spatial pattern of net primary productivity in Chinese forests. Ecol. Model. 122, 275–288.
Jolliffe, I.T., 2002. Principal Component Analysis, second ed. Springer, New York.
Juan, J., Prieto, F.J., 2001. Using angles to identify concentrated multivariate outliers. Technometrics 43, 311–322.
Karau, E., Keane, R.E. Determining the spatial extent of a landscape using simulation modeling. Landscape Ecol., submitted for publication.
Keane, R.E., Long, D.G., Menakis, J.P., Hann, W.J., Bevins, C.D., 1996. Simulating coarse-scale vegetation dynamics using the Columbia River Basin succession model: CRBSUM. USDA Forest Service Intermountain Research Station, Ogden, UT.
Keane, R.E., Austin, M., Dalman, R., Field, C., Huth, A., Lexer, M., Peters, D., Solomon, A., Wycoff, P., 2001. Tree mortality in gap models: application to climate change. Climatic Change 51, 509–540.
Keane, R.E., Parsons, R., Hessburg, P., 2002a. Estimating historical range and variation of landscape patch dynamics: limitations of the simulation approach. Ecol. Model. 151, 29–49.
Keane, R.E., Veblen, T., Ryan, K.C., Logan, J., Allen, C. Hawkes, B., 2002b. The cascading effects of fire exclusion in the Rocky Mountains. In J. Baron (Ed.), Rocky Mountain Futures: An Ecological Perspective, Island Press, Washington DC, USA. 133–153.
Keane, R.E., Cary, G.J., Davies, I.D., Flannigan, M.D., Gardner, G.H., Lavorel, S., Lenihan, J.M., Li, C., Rupp, T.S., 2004. A classification of landscape fire succession models: spatial simulations of fire and vegetation dynamics. Ecol. Model. 179, 3–27.
Keane, R.E., Holsinger, L., Pratt, S., 2006. Simulating historical landscape dynamics using the landscape fire succession model LANDSUM Version 4.0. USDA Forest Service General Technical Report INT-171CD. USDA Forest Service Rocky Mountain Research Station, Fort Collins, CO, USA.
Kolb, P.F., Adams, D.L., McDonald, G.I., 1998. Impacts of fire exclusion on forest dynamics and processes in central Idaho. Tall Timbers Fire Ecol. Conf. 20, 911–923.
Landres, P.B., Morgan, P., Swanson, F.J., 1999. Overview and use of natural variability concepts in managing ecological systems. Ecol. Appl. 9, 1179–1188.
Laverty, L. Williams, J., 2000. Protecting people and sustaining resources in fire-adapted ecosystems—a cohesive strategy. Forest Service Response to GAO Report GAO/RCED, 99–65. USDA Forest Service, Washington, DC.
Long, D.G., Losensky, J., Bedunah, D. Vegetation succession modeling for the LANDFIRE prototype project. In: Rollins, M.G., Frame, C.K. (Eds.), The LANDFIRE Prototype Project: Nationally Consistent and Locally Relevant Geospatial Data for Wildland Fire Management. USDA Forest Service Rocky Mountain Research Station General Technical Report RMRS-GTR-175, Fort Collings, CO, USA, in press.
Mladendoff, D.J., Baker, W.L., 1999. Spatial Modeling of Forest Landscape Change: Approaches and Applications. Cambridge Univ. Press, Cambridge, UK, p. 329.
Nour, M.H., Smith, D.W., Gamal El-Din, M., Prepas, E.E., 2006. The application of artificial neural networks to flow and phosphorus dynamics in small streams on the Boreal Plain, with emphasis on the role of wetlands. Ecol. Model. 191, 19–32.
Pena, D., Preito, F.J., 2001. Multivariate outlier detection and robust covariance matrix estimation (with discussion). Technometrics 43, 286–310.
Penny, K.I., Jolliffe, I.T., 2001. A comparison of multivariate outlier detection methods for clinical laboratory safety data. Statistician 50, 295–308.
Pfister, R.D., Arno, S.F., 1980. Classifying forest habitat types based on potential climax vegetation. Forest Sci. 26, 52–70.
Ott, R.L., Longnecker, M., 2001. An Introduction of Statistical Methods and Data Analysis, fifth ed. Duxbury, Pacific Grove, CA.
Rao, C.R., 2004. Statistics: reflections on the past and visions of the future. AMSTAT News 327, 2–3.
Rothermel, R.C., 1991. Predicting behavior and size of crown fires in the Northern Rocky Mountains. USDA Forest Service Research Paper, INT-438, Ogden, UT, USA.
Schott, J.R., 1997. Matrix Analysis for Statistics. Wiley, New York.
Vogel, C.R., 2002. Computational Methods for Inverse Problems. SIAM, Philadelpia.
Waring, R.H., Running, S.W., 1998. Forest Ecosystems: Analysis at Multiple Scales, second ed. Academic Press, San Diego.
Wright, H.E., Heinselman, M.L., 1973. Introduction: ecological role of fire. Quaternary Res. 3, 319–328.